

See discussions, stats, and author profiles for this publication at: <https://www.researchgate.net/publication/261874621>

Poly (3, 4-ethylenedioxythiophene) Hole Transporting Material Generated by Photoelectrochemical Polymerization in Aqueous and Organic Medium for All-Solid State Dye Sensitized Sola...

ARTICLE in THE JOURNAL OF PHYSICAL CHEMISTRY C · APRIL 2014

Impact Factor: 4.77 · DOI: 10.1021/jp412504s

CITATIONS

7

READS

207

15 AUTHORS, INCLUDING:



Byung-wook Park

Ulsan National Institute of Science and Techn...

25 PUBLICATIONS 257 CITATIONS

SEE PROFILE



Yan Hao

Uppsala University

27 PUBLICATIONS 472 CITATIONS

SEE PROFILE



Gerrit Boschloo

Uppsala University

197 PUBLICATIONS 14,077 CITATIONS

SEE PROFILE



Christian Perruchot

Paris Diderot University

50 PUBLICATIONS 1,560 CITATIONS

SEE PROFILE

Poly(3,4-ethylenedioxythiophene) Hole-Transporting Material Generated by Photoelectrochemical Polymerization in Aqueous and Organic Medium for All-Solid-State Dye-Sensitized Solar Cells

Jinbao Zhang,^{†,‡} Lei Yang,^{†,‡} Yang Shen,[†] Byung-Wook Park,[†] Yan Hao,[†] Erik M. J. Johansson,[†] Gerrit Boschloo,[†] Lars Kloo,[‡] Erik Gabrielsson,^{||} Licheng Sun,^{||} Adel Jarboui,[§] Christian Perruchot,[§] Mohamed Jouini,[§] Nick Vlachopoulos,^{*,†} and Anders Hagfeldt^{†,§,⊥}

[†]Department of Chemistry-Ångström Laboratory, Uppsala University, 75120 Uppsala, Sweden

[‡]Applied Physical Chemistry, Department of Chemistry, KTH-Royal Institute of Technology, Teknikringen 30, SE-10044 Stockholm, Sweden

[§]Université Paris Diderot Paris 7, Sorbonne Paris Cité, ITODYS UMR 7086 CNRS, 15 rue Jean-Antoine de Baïf, 75205 Paris Cedex 13, France

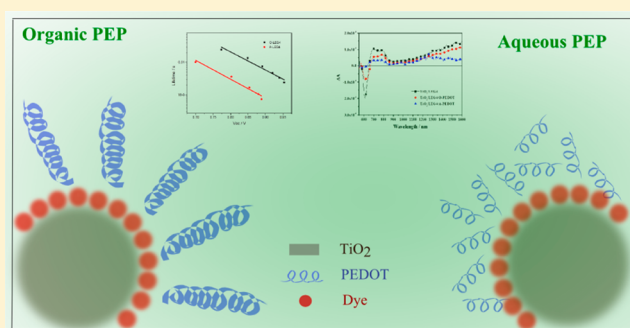
^{||}Organic Chemistry, Department of Chemistry, KTH-Royal Institute of Technology, Teknikringen 30, SE-10044 Stockholm, Sweden

[⊥]School of Chemical Engineering, Sungkyunkwan University, Suwon 440-746, Korea

Supporting Information

ABSTRACT: We applied organic donor- π -acceptor (D- π -A) sensitizers for photoelectrochemical polymerization (PEP) because of their appropriate energy levels and high light absorption. The polymerized conducting polymer PEDOT was used as hole conductor in all-solid-state dye-sensitized solar cells (ssDSCs). By combination of the D- π -A sensitizers and the generated PEDOT from PEP of *bis*-EDOT in acetonitrile, the resulting device showed an average power conversion efficiency of 5.6%. Furthermore, the PEP in aqueous micellar electrolytic medium was also employed because of the ability to decrease oxidation potential of the precursor, thereby making the polymerization process easier.

The latter method is a cost-effective and environmentally friendly approach. Using as hole conductor the so-obtained PEDOT from PEP of *bis*-EDOT in aqueous electrolyte, the devices exhibited impressive power conversion efficiency of 5.2%. To compare the properties of the generated polymer from *bis*-EDOT in these two PEP methods, electron lifetime, photoinduced absorption (PIA) spectra, and UV-vis-NIR spectra were measured. The results showed that PEDOT from organic PEP exhibits a delocalized conformation with high conductivity and a smooth and compact morphology; a rough morphology with high porosity and polymer structure of relatively shorter chains was assumed to be obtained from aqueous PEP. Therefore, better dye regeneration but faster charge recombination was observed in the device based on PEDOT from aqueous PEP of *bis*-EDOT. Subsequently, to extend the aqueous PEP approach in consideration of the ability to decrease the oxidation potential of the precursor, the easily available precursor EDOT was for the first time used for PEP in aqueous medium in a variant of the aforementioned procedure, and the device based on the so-obtained PEDOT shows a more than 70-fold increase in efficiency, 3.0%, over that based on the polymer generated from EDOT by PEP in organic media. It was demonstrated that aqueous micellar PEP with EDOT as monomer is an efficient strategy for generation of conducting polymer hole-transporting materials.



1. INTRODUCTION

Dye-sensitized solar cells (DSCs) have exhibited great potential as energy conversion devices for providing a sustainable electricity source from the sun because of their low fabrication costs, good stability, and promising conversion efficiency. The first fundamental studies on efficient high surface area TiO₂ electrode sensitization were made in the 1980s and then followed by the seminal work in 1991 by O' Regan and Grätzel on the first efficient electricity-producing DSCs based on colloidal TiO₂ layers.^{1–3} DSCs consist of an n-type electronic

conductor, typically porous semiconductor titanium dioxide, sensitized by a monolayer of sensitizer and filled with a charge-transport medium, either an electrolyte containing a redox mediator, in liquid or solid polymer electrolyte-based DSCs, or

Special Issue: Michael Grätzel Festschrift

Received: December 20, 2013

Revised: April 8, 2014

a solid hole-transporting material (HTM) in solid-state DSCs (ssDSCs).^{4–6} Charge separation can occur at the interface by injection of electrons from the photoexcited sensitizer into the conduction band of the semiconductor oxide.⁷ Subsequently, the sensitizer in the oxidized form can be regenerated by the surrounding hole transporter. Therefore, the charge-transport medium is one of the most critical components in DSCs, affecting the rate of dye regeneration, determining the photovoltage of DSCs system, and therefore playing a key role in the photoconversion efficiency. Several types of redox couple-based liquid DSCs have shown above 10% energy conversion efficiency.^{8–10} However, liquid DSCs may suffer from electrolyte leakage, electrode corrosion, and long-term stability. Therefore, solid-state hole-transporting materials, replacing the liquid electrolyte, have attracted a lot of attention.^{11–13}

Spiro-OMeTAD has been one of most popular and favorable HTMs because of good solubility in common solvents and easy fabrication process by spin coating.^{14–16} However, it has low conductivity ($10^{-4} \text{ cm}^2 \text{ V}^{-1} \text{ s}^{-1}$), high cost, and poor infiltration in metal oxide pores, thereby limiting the large-scale application of ssDSCs.¹⁷ This has motivated different research groups to search for new alternative HTMs.^{18–21} Among the various options, conjugated polymers have been widely investigated as potential HTMs in ssDSCs because they have high conductivity, great thermal stability, and switchable optical and redox properties.²² In this respect poly(3, 4-ethylenedioxythiophene), namely, PEDOT, has been the most outstanding representative polymer hole conductor. Initially, a rather poor photoconversion efficiency was obtained using the so-called Ru-N719 dye because of strong interfacial electron recombination.²³ When the doping anions of PEDOT were optimized, a great enhancement of photovoltaic performance was obtained by using the anion TFSI[−] as dopant and, initially, Ru-Z907 as sensitizer.²⁴ In further studies, to suppress the high interfacial charge recombination and control polymer penetration, an organic indoline-type dye, D149, was efficiently used with PEDOT as HTM in ssDSCs, and the corresponding device showed a promising efficiency of 6.1%.²⁵

Because of the low solubility of PEDOT and to improve its contact as HTM with dye molecules, in situ photoelectrochemical polymerization (PEP) is the most common method of generating a PEDOT film at the dye/TiO₂ electrode interface.^{21,26–28} During PEP, irradiation by light can excite the sensitizer, and the oxidized dye molecules can work as active sites to initiate and maintain the polymerization reaction. Photogenerated holes on the highest occupied molecular orbital (HOMO) level of dyes can oxidize the precursor and trigger oxidized precursor coupling. Hence, the choice of both employed precursor and dye sensitizer significantly influences the polymerization process. At first glance, one of the critical requirements for the dye sensitizers would be that they should have a more positive redox potential ($E^\circ_{\text{Dye}^+/\text{Dye}}$) than the onset oxidation potential of the precursor (E_{onset}) because this potential difference could be considered as a kind of driving force of PEP, determining the rate of polymerization process and the properties of the polymer produced inside the TiO₂ pores. Another consideration of dye sensitizers is that there is often a trade-off between a wide absorption spectra range and a high extinction coefficient, both of which affect the ability to utilize the light. In this work, different donor- π -acceptor (D- π -A)-based sensitizers were applied to polymerize suitable precursors to get a regular polymer²⁹ by choosing the dyes

with proper energy levels and light absorption ability because of the fact that π -units in the D- π -A structure are used to control the HOMO–LUMO gap, which can determine the photon absorption edge.³⁰ Beyond that, another way to engender efficient PEP is to use a precursor with a proper onset oxidation potential. Initially, pyrrole was used as precursor; however, this lead to a nontransparent polymer.^{31,32} Recently, 3,4-ethylenedipyrrole (EDOP) has been reported for the first time as a precursor of PEP by combination with D- π -A-based sensitizers, which gives 3.0% efficiency by efficient suppression of charge recombination.²¹ *bis*-EDOT (2,3-dihydro-5-(2,3-dihydrothieno[3,4-*b*][1,4]dioxin-5-yl)thieno[3,4-*b*][1,4]dioxine)^{23–25,33–35} has been mostly used as precursor for PEP in organic media because of its low oxidation potential compared to the redox potentials of the dyes; *bis*-EDOT is also preferred because of its higher reactivity and solubility as compared to that of the alternative triethylenedioxythiophene (*tri*-EDOT). In this work, *bis*-EDOT was employed as precursor of PEDOT, and by combination of D- π -A-based sensitizers and PEDOT HTM, the devices show excellent photovoltaic performance, with an average power conversion efficiency of 5.6%.

Moreover, to have a lower electrochemical polymerization potential of the precursor, PEP in aqueous micellar electrolyte was employed;²⁹ additional advantages in aqueous medium are low cost and environmental compatibility.^{36–42} At present, by using aqueous PEP of the precursor *bis*-EDOT, the generated PEDOT-based devices with a D- π -A sensitizer show the impressive photoconversion efficiency of 5.2%.

In addition, to extend the aqueous PEP approach, the one-unit precursor EDOT was employed for the first time as precursor for in situ PEP to generate PEDOT instead of *bis*-EDOT because EDOT can be oxidized at lower potential when water is used as solvent, compared with that in organic medium. In this work both an organic and an aqueous PEP medium were investigated. The devices based on PEDOT obtained from EDOT as precursor and D- π -A sensitizer in these two media exhibited power conversion efficiency of 0.04% and 3.0%, respectively. The high efficiency of the device based on PEP of EDOT in aqueous solvent may result from a more efficient polymerization reaction in this medium.

2. EXPERIMENTAL SECTION

2.1. Chemicals Used. All chemicals were purchased from Sigma-Aldrich unless otherwise indicated. *Bis*-EDOT (K192, Kairon Chemicals, France) was used for photoelectrochemical polymerization. Dyes D35 and LEG4 were supplied by Dyenamo AB (Sweden).^{43,44} Z907 was purchased from Dyesol (Australia).

2.2. Device Fabrication. The fluorine-doped SnO₂ (FTO, 15 Ω -square) substrates were etched with zinc powder and HCl (concentration 3 M) to form the desired electrode pattern. The substrates were cleaned in an ultrasonic bath for 30 min in the following order: deionized water, acetone, and ethanol. A compact layer of TiO₂, intended to block the recombination current at the FTO support, was prepared on cleaned FTO substrate by spray pyrolysis according to the published procedure.⁴⁵ To generate the porous, dye-adsorbing TiO₂ layer, the colloidal TiO₂ paste was doctor-bladed on the compact layer surface then sintered by a stepwise heating process: 180 °C for 10 min, 320 °C for 10 min, 400 °C for 10 min, and 450 °C for 30 min in an oven (Nabertherm Controller P320) in air atmosphere to form the nanoporous TiO₂ film. After the sintering was complete, the films were

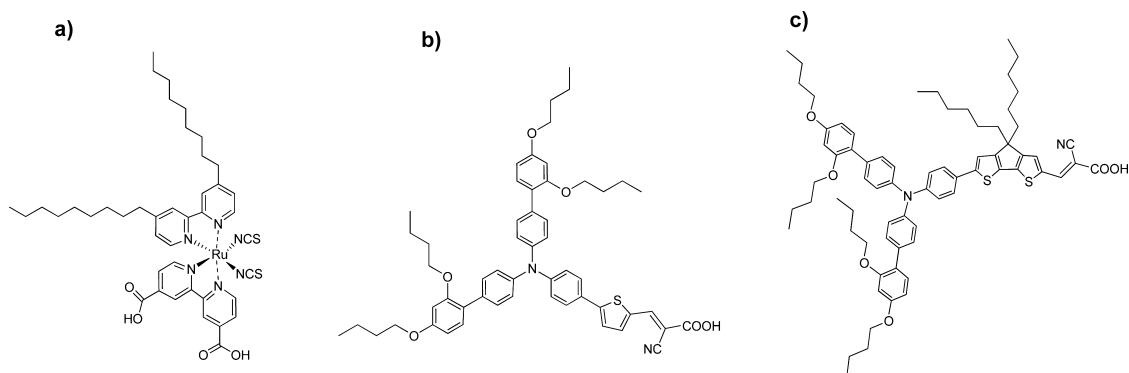


Figure 1. Chemical structures of different sensitizers (a) Z907, (b) D35, and (c) LEG4.

treated with 40 mM TiCl_4 aqueous solution at 70 °C for 30 min; in this way an overlayer is formed, increasing the roughness factor and therefore the dye uptake. After subsequent rinsing with deionized water and ethanol, the film was sintered again by following the aforementioned procedure. After being cooled to 90 °C, the hot TiO_2 film was immersed into the dye solution for 18 h. The dyes used for this purpose were the ruthenium dye Ru-Z907 (0.2 mM in a mixture of acetonitrile and *tert*-butyl alcohol, v/v 1:1) and two metal-free organic dyes: D35 (0.2 mM in ethanol) and LEG4 (0.2 mM in a mixture of acetonitrile and *tert*-butyl alcohol, v/v 1:1). The dye structures are shown in Figure 1. The films were rinsed in ethanol and dried by a N_2 gas flow. The dye-sensitized TiO_2 layer was covered by the hole-transporting material PEDOT by means of PEP. After polymerization, the electrode was carefully washed and then underwent a post-treatment procedure by one drop of solution consisting of 0.02 M $\text{LiN}(\text{CF}_3\text{SO}_2)_2$ and 0.2 M 4-*tert*-butylpyridine (TBP) in acetonitrile. Finally, after removal of remaining acetonitrile by drying, a 200 nm thick Ag (Sigma-Aldrich; $\geq 99.99\%$ trace metals basis) contact layer, forming the dark counter electrode of the device, was deposited onto the PEDOT organic semiconductor layer, covering the dye-sensitized TiO_2 electrode, by thermal evaporation in a vacuum chamber (Leica EM MED020) with a base pressure of about 10^{-5} mbar to complete the device.

2.3. Photoelectrochemical Polymerization (PEP). A three-electrode cell was employed for PEP. The FTO substrates supporting the dye-sensitized TiO_2 layers were used as working electrodes. The counter electrode and reference electrode were stainless steel and aqueous Ag/AgCl (3 M NaCl), respectively. Two alternative electrolytes for polymerization of *bis*-EDOT were chosen: (a) organic electrolyte, with 10 mM *bis*-EDOT and 0.1 M $\text{LiN}(\text{CF}_3\text{SO}_2)_2$ in acetonitrile, and (b) aqueous micellar electrolyte, a saturated solution of *bis*-EDOT (solubility below 1 mM) in an aqueous solution containing 2% v/v acetonitrile, 0.1 M $\text{LiN}(\text{CF}_3\text{SO}_2)_2$, and 50 mM TritonX-100 surfactant as solubilization medium. For the nonaqueous PEP of EDOT, a solution of 10 mM EDOT and 0.1 M $\text{LiN}(\text{CF}_3\text{SO}_2)_2$ in acetonitrile was used. For the aqueous PEP, an aqueous solution containing 10 mM EDOT, 50 mM TritonX-100, and 100 mM $\text{LiN}(\text{CF}_3\text{SO}_2)_2$ was used. The white light was provided by a LED lamp (ELFA Distrelec, Light Injector, white, 6000 K-6°, 3 W, 4.5 V, 700 mA). The illumination was from the back (glass) side of the FTO/ TiO_2 layer. For the nonaqueous polymerization of *bis*-EDOT with the dye LEG4/ TiO_2 and dye D35/ TiO_2 electrodes, a current density of $8 \mu\text{A cm}^{-2}$ was applied for 1500 s; for the nonaqueous polymerization of EDOT with the dye D35/

TiO_2 electrode, the same current density of $8 \mu\text{A cm}^{-2}$ was applied for 2000 s; and for the nonaqueous polymerization with the dye Ru-Z907/ TiO_2 , $6 \mu\text{A cm}^{-2}$ and 3000 s. For the aqueous micellar polymerization of *bis*-EDOT with dye LEG4/ TiO_2 and dye D35/ TiO_2 , the respective conditions were $6 \mu\text{A cm}^{-2}$ and 2000 s; for aqueous micellar polymerizations of EDOT with dye LEG4/ TiO_2 and dye D35/ TiO_2 , $6 \mu\text{A cm}^{-2}$ and 2500 s were used, respectively. The electrode potential was monitored against the reference electrode so that it did not overstep a stipulated positive potential limit, 0.6 V_{SHE} (standard hydrogen electrode), to prevent both the overoxidation of the formed conducting polymer and its generation at sites where the underlayer could be damaged; in the latter case the FTO substrate could be directly exposed to the electrolyte. After the electrolyte was rinsed off, the films were washed using ethanol and then dried by N_2 flow.

2.4. Electrochemical Measurement. A three-electrode electrochemical cell was used for the cyclic voltammetry experiments. The supporting electrolyte for electrochemical measurements was either (a) organic electrolyte, 0.1 M $\text{LiN}(\text{CF}_3\text{SO}_2)_2$ in acetonitrile, or (b) aqueous electrolyte, 0.1 M $\text{LiN}(\text{CF}_3\text{SO}_2)_2$ and 50 mM Triton X-100 in water. In all cases, stainless steel was used as the counter electrode with an area of 3 cm². The reference electrode was in all cases aqueous Ag/AgCl/3 M NaCl; a salt bridge electrolyte was interposed between the working and reference electrode, containing 0.1 M $\text{LiN}(\text{CF}_3\text{SO}_2)_2$ in water or acetonitrile, depending on the working electrode solvent. For experiments in organic electrolyte, the reference electrode was calibrated with ferrocene in 1 M KCl; the literature value of 0.624 V_{SHE} was used for conversion of potential values.⁴⁶ For the experiments in aqueous medium, the reference electrode was calibrated with ferricyanide in the same electrolyte, for the redox potential of which the literature value of 0.471 V_{SHE} (or 0.266 V_{SCE}, versus the standard calomel electrode) was used for conversion of potential values.⁴⁷ All potentials are reported versus SHE. For measurements of the oxidation potentials of *bis*-EDOT in (a) organic and (b) aqueous solution, a glassy carbon disk ($d = 3$ mm) was used as working electrode, which was carefully polished with 0.05 μm alumina slurry before every experiment. For measurements of dye redox potentials, the dye was chemisorbed at mesoporous TiO_2 /FTO electrodes (area of 1 cm²) without blocking compact underlayer; dye/ TiO_2 /FTO served as the working electrode for redox potential determination.

2.5. Solar Cell Characterization. Current–voltage characteristics were measured under 100 mW cm^{−2} (AM 1.5G illumination) using a Newport solar simulator (model 91160)

and a Keithley 2400 source-meter. A certified reference solar cell (Fraunhofer ISE) was used to calibrate the light source for an intensity of 100 mW cm^{-2} . A black mask with a 0.20 cm^2 aperture area ($0.4 \times 0.5 \text{ cm}^2$), yielding the solar cell active area, was positioned on the top of the cell during the measurement. Incident photon-to-current conversion efficiency (IPCE) spectra were recorded using a computer-controlled setup consisting of a Xenon light source (Spectral Products ASB-XE-175), a monochromator (Spectra Products CM110), and a potentiostat (EG&G PAR 273) calibrated by a certified reference solar cell (Fraunhofer ISE). Electron lifetime measurements were performed using a white LED (Luxeon Star 1W) as the light source. The electron lifetime was determined by monitoring photovoltage transients at different light intensities by applying a small square-wave modulation to the base light intensity. The photovoltaic response was fitted using first-order kinetics to obtain time constants.

2.6. Photoinduced Absorption Spectroscopy. Photoinduced absorption (PIA) measurements were carried out on solar cell device samples, prepared as described above, without either the post-treatment or the Ag contact layer. Photosensitized samples without a HTM were also investigated. PIA spectra were recorded on the homemade setup as reported previously.⁴⁸ White probe light generated by a 20 W tungsten–halogen lamp was filtered up to 530 nm and was superimposed on a square-wave modulated (on–off) green light source (Lasermate GMLS32–100FLE, 532 nm) used for excitation. The transmitted probe light was focused onto a monochromator (Action Research Corporation SP-150) and detected by a UV-enhanced silicon (visible region) and germanium (NIR–IR region) photodiode detector connected to a current amplifier and lock-in amplifier (Stanford Research System models RS570 and RS830, respectively). The intensity of 6.1 mW cm^{-2} and modulation frequency of 9.3 Hz were used for the excitation blue LED.

2.7. UV–vis–NIR Spectra Measurement. To measure UV–vis–NIR absorption spectra, the dye-sensitized TiO_2 electrodes, with and without PEDOT, were prepared according to the procedure described in Section 2.2. The measurement was performed on a Cary 5000 UV–vis–NIR spectrophotometer (VARIAN; photometric accuracy is $\leq 0.00025 \text{ Abs.}$; photometric range is 8 Abs.). The FTO/ TiO_2 substrate signal was used as calibration background.

2.8. Hole Conductivity and Mobility Measurement. Devices for hole conductivity and mobility of PEDOT were prepared following the fabrication procedures of solar cells but without post-treatment. Measurements were carried out between two deposited silver counter electrodes on the back side of the devices under dark conditions. Electrical data were recorded on a computer-controlled digital source-meter (Keithley Model 2400) with the scan direction from -2.5 V to $+2.5 \text{ V}$ at 50 mVs^{-1} . The distance and the area between two silver counter electrodes were 2 mm and 0.1 cm^2 , respectively.

3. RESULTS AND DISCUSSION

3.1. Electrochemical Measurement. To conduct efficient PEP, one of the most basic requirements for a sensitizer is that its redox potential (vs SHE) should be more positive than the onset oxidation potential of the precursor. Electrochemical measurements were carried out to compare the potential values of different dyes (Ru-Z907, D35, and LEG4, in Figure 1) and the precursor *bis*-EDOT and EDOT.

The cyclic voltammetry curve of *bis*-EDOT in acetonitrile-based electrolyte is shown in Figure SI-1a of the Supporting Information. The onset oxidation potential of *bis*-EDOT at 10^{-2} M is $0.9 \text{ V}_{\text{SHE}}$. Cyclic voltammetry curves in organic medium of three dyes, LEG4, D35, and Ru-Z907, on TiO_2 film were also investigated, as shown in Figure SI-1d,e of the Supporting Information. The redox potentials for LEG4 and D35 are $1.06 \text{ V}_{\text{SHE}}$ and $1.16 \text{ V}_{\text{SHE}}$, respectively. For Z907, the redox potential is $1.05 \text{ V}_{\text{SHE}}$, as shown in Figure SI-1d of the Supporting Information. The redox potential of each dye is higher than the onset oxidation potential of the *bis*-EDOT electrochemical polymerization at a conductive substrate in an acetonitrile-based electrolyte, which demonstrates that these three dyes can be used for PEP of *bis*-EDOT in an organic electrolyte. The onset oxidation potential of *bis*-EDOT ($<1 \text{ mM}$) is $0.6 \text{ V}_{\text{SHE}}$ in the aqueous phase, which is $0.3 \text{ V}_{\text{SHE}}$ lower than that in acetonitrile-based electrolyte, as indicated in Figure SI-1b of the Supporting Information. The redox potentials in aqueous electrolyte of LEG4 and D35 immobilized on a TiO_2 film, as measured by cyclic voltammetry (Figure SI-1f of the Supporting Information), are $0.8 \text{ V}_{\text{SHE}}$ and $0.9 \text{ V}_{\text{SHE}}$, respectively. These values indicate that these two D- π -A sensitizers are proper candidates for PEP in aqueous electrolyte. For the precursor EDOT, its onset oxidation potentials at 10 mM in organic medium and in aqueous medium (Figure SI-1c of the Supporting Information) are $1.6 \text{ V}_{\text{SHE}}$ and $0.9 \text{ V}_{\text{SHE}}$, respectively. The detailed values of potentials for all species relevant to the present studies are summarized in Table 1.

Table 1. Redox Potential Values versus SHE for the Sensitizers Z907, D35, and LEG4 Films Deposited on TiO_2 , and Onset Oxidation Potential Values for precursors *bis*-EDOT and EDOT in Aqueous and Nonaqueous Electrolyte, Measured Using a 3 mm Diameter Glassy Carbon Disk as Working Electrode

	<i>bis</i> -EDOT	EDOT	LEG4	D35	Z907
medium	E_{onset} (V_{SHE})	E_{onset} (V_{SHE})	E_{redox} (V_{SHE})	E_{redox} (V_{SHE})	E_{redox} (V_{SHE})
organic	0.90	1.60	1.06	1.16	1.05
aqueous	0.60	0.90	0.80	0.90	–

As can be seen from Table 1, both the onset potentials of *bis*-EDOT, EDOT, and the redox potentials of D35 and LEG4 decrease in an aqueous electrolyte compared with the values obtained in an organic electrolyte. Moreover, the redox potentials of D- π -A sensitizers used in this study are more positive than the onset oxidation potential of *bis*-EDOT, both in aqueous and organic electrolyte, which indicates that D- π -A dyes can be efficiently used for PEP in both media. As far as PEP of EDOT is concerned, the redox potential of D35 is very close to the onset oxidation potential of EDOT in aqueous medium; the redox potential of LEG4 is somewhat less positive than the onset of EDOT oxidation, indicating less favorable PEP conditions. PEP of EDOT in organic medium is not thermodynamically feasible.

As regards Ru-Z907, the attachment on TiO_2 is unstable in aqueous electrolytes, which can be confirmed from the fact that Ru-Z907 is dissolved into the aqueous electrolyte during PEP experiments. Thus, this dye is not suitable to be used for efficient PEP in aqueous solution.

3.2. Photovoltaic Properties of ssDSCs Based on PEDOT HTM from Precursor *bis*-EDOT. To investigate the device performance by combination of D- π -A sensitizers and polymerization of the precursor *bis*-EDOT for ssDSCs in the two different media, two groups of devices were fabricated with the configurations shown in Figure 2, which are marked as O-

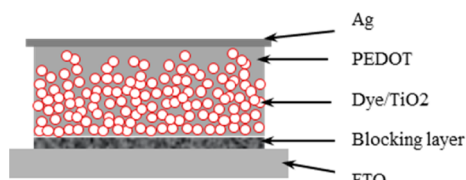


Figure 2. Schematic structure of PEDOT HTM-based ssDSCs devices.

dye (combination of dyes and PEDOT-based on organic PEP) and A-dye (dyes and PEDOT-based on aqueous PEP), respectively. For comparison, the Ru-complex Ru-Z907 was also used to generate PEDOT by PEP in both media by following the same fabrication process.

I–*V* curves of devices O-LEG4, O-D35 and O-(Ru-Z907), are shown in Figure 3a. Table 2 summarizes the detailed photovoltaic parameters of these devices. For the device of O-LEG4, a short circuit current (J_{sc}) of 10.80 mA cm^{−2}, an open circuit voltage (V_{oc}) as high as 0.91 V, and a fill factor (*ff*) of 0.57 were obtained, yielding a total power conversion efficiency (η) of 5.6%. For the device of O-D35, η = 4.6% was obtained, with J_{sc} of 8.19 mA cm^{−2}, V_{oc} of 0.83 V, and *ff* of 0.68. In contrast, a lower η of 1.5%, with J_{sc} of 4.49 mA cm^{−2}, V_{oc} of 0.51 V, and *ff* of 0.66, was observed in the O-Z907 device; these values for O-Z907 are similar to those reported in the literature.²⁵

The devices based on PEDOT generated by aqueous polymerization and the three aforementioned sensitizers were fabricated following the same procedures. Figure 3b shows the *I*–*V* curves of corresponding devices with dyes A-LEG4 and A-D35. It can be seen that a typically high photovoltaic performance with η up to 5.2% power efficiency was achieved in the case of the A-LEG4-based device. The values of J_{sc} = 10.94 mA cm^{−2} (close to that for the O-LEG4-based device), V_{oc} = 0.84 V (lower by 0.07 V compared to that for O-LEG4 case), and *ff* of 0.56 (lower than that of O-LEG4) lead to the impressive photoconversion efficiency. As for the A-D35, it showed a J_{sc} = 8.60 mA cm^{−2}, low V_{oc} of 0.78 V, lower *ff* of 0.56, and a power efficiency of 3.8% (compared to 4.6% for O-D35). The comparison of the fill factors of different devices, A-LEG4 and O-LEG4, A-D35 and O-D35, agrees with the fact that a higher charge-transport related resistance was expected for devices based on the aqueous PEP-based PEDOT compared to the organic PEP-based PEDOT, which results from the lower hole conductivity and mobility, as discussed in Section 3.7.

However, a notably poorer photovoltaic performance compared to the above systems was obtained for the device based on A-(Ru-Z907). Note that there is almost no polymer in the Z907/TiO₂ film after PEP; this is due to the observed dissolution of a large amount of dye Z907 into the aqueous electrolyte during PEP, despite the oxidation of *bis*-EDOT which takes place at the same time.

3.3. Photovoltaic Properties of ssDSCs Based on PEDOT HTM from Precursor EDOT. In consideration of the decreased oxidation potential of the precursor in aqueous

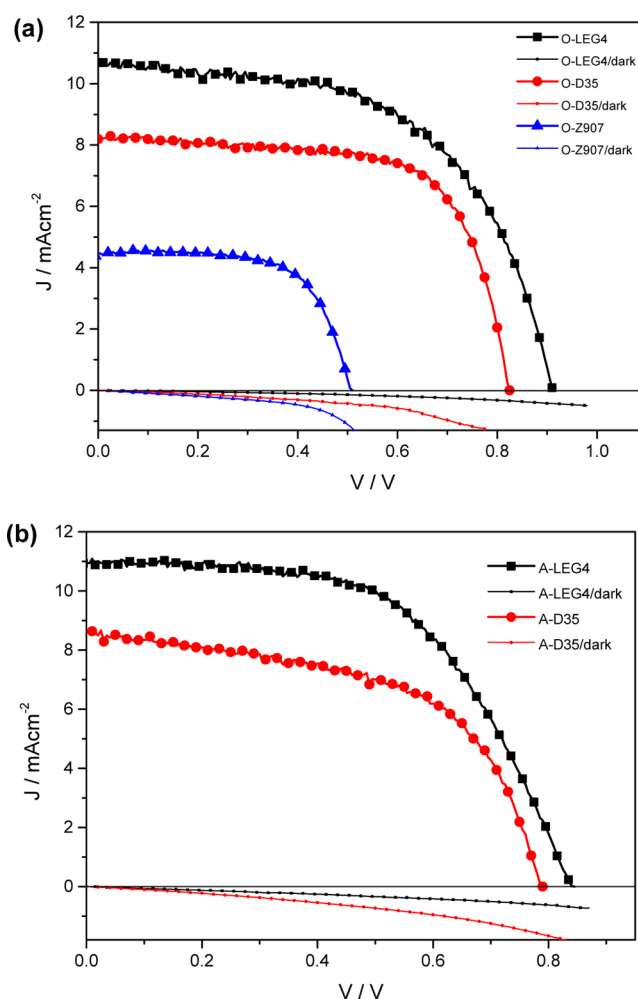


Figure 3. Current–voltage characteristics of solar cell based on (a) PEDOT generated from organic electrolyte and (b) PEDOT generated from aqueous-based electrolyte, measured under a light intensity of 100 mW cm^{−2} (large dots and squares) and in the dark (small dots and squares).

Table 2. Photovoltaic Parameters of Devices Based on PEDOT from PEP of *bis*-EDOT in Organic and Aqueous Media with Different Dyes

	medium	η (%)	V_{oc} (V)	J_{sc} (mA cm ^{−2})	<i>ff</i>
LEG4	organic	5.6	0.91	10.80	0.57
	aqueous	5.2	0.84	10.94	0.56
D35	organic	4.6	0.83	8.19	0.68
	aqueous	3.8	0.78	8.60	0.56
Z907	organic	1.5	0.51	4.49	0.66
	aqueous	0.07	0.42	0.45	0.39

electrolyte, EDOT was for the first time tested as precursor for PEP to generate PEDOT in an aqueous medium; for comparison, the PEP of EDOT in organic electrolyte is also discussed here. Because the onset oxidation potential of EDOT is 1.6 V_{/SHE}, much higher than the redox potential of sensitizers considered in this work, an inefficient performance of the PEP process is expected to occur in organic medium, leading probably to PEDOT with very short, if any, chains deposited on the dye-modified TiO₂ electrode surface and causing a large series resistance in the device and slow regeneration of sensitizers. This explains why the devices with PEDOT from

organic PEP show poor performance, $\eta = 0.04\%$, as shown in Table 3. In contrast, PEP of EDOT in aqueous electrolyte was

Table 3. Photovoltaic Parameters of Devices Based on PEDOT from PEP of EDOT in Organic and Aqueous Media with Sensitizer D35 at a Light Intensity of 100 mW cm^{-2}

	η (%)	V_{oc} (V)	J_{sc} (mA cm^{-2})	ff
O-D35	0.04	0.62	0.27	0.25
A-D35	3.03	0.81	6.20	0.60

employed to prepare a PEDOT hole conductor because of the lower onset oxidation potential of $0.9 \text{ V}_{\text{SHE}}$ for EDOT in the aqueous phase. The sensitizer D35 was initially chosen because it has oxidation potential comparable with that of EDOT. Surprisingly, the combination of D35 and EDOT precursor made it possible to perform in situ PEP of EDOT in this medium quite efficiently. The photovoltaic performances of the corresponding devices are shown in Figure 4.

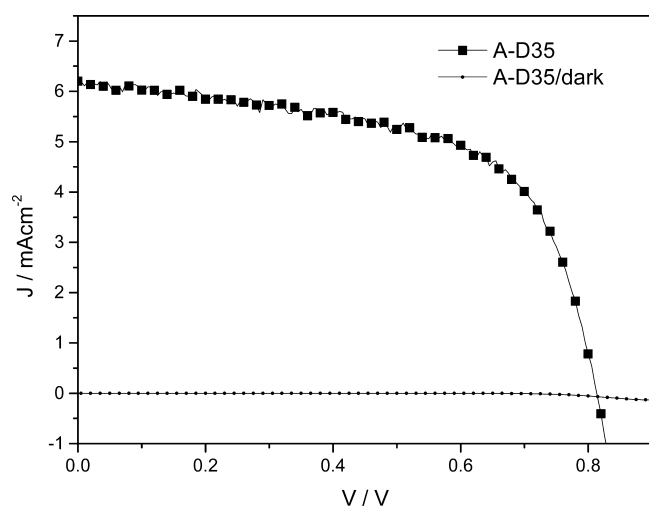


Figure 4. I – V curves of devices based on dye D35 and PEDOT from PEP of EDOT in aqueous electrolyte under light intensity of 100 mW cm^{-2} (large squares) and in the dark (small squares).

Table 3 shows the detailed photovoltaic parameters of devices using D35 and PEDOT from precursor EDOT in organic and aqueous PEP. As expected, the O-D35 showed poor photovoltaic performance with a low photocurrent of 0.27 mA cm^{-2} . Much better performance with $\eta = 3.0\%$, with V_{oc} of 0.81 V , J_{sc} of 6.20 mA cm^{-2} , and ff of 0.60 , was obtained by combination of PEDOT from aqueous PEP of EDOT and dye D35 under a light intensity of 100 mW cm^{-2} . The above data clearly indicates that PEP in aqueous medium is an efficient method for polymer-based HTM preparation, provided that the efficient combination of the redox potential of the dye and the onset oxidation potential of the precursor is found.

3.4. Incident Photon-to-Current Conversion Efficiency and Light Absorption Measurement. Figure 5 shows the corresponding incident photon-to-current conversion efficiency (IPCE) spectra for the devices based on O-dyes (Figure 5a) and A-dyes (Figure 5b). The IPCE data agree well with the J_{sc} values shown in Table 2. The maximum IPCE of O-LEG4-based device (80% at 470 nm) corresponds to a higher and broader absorption than that of the O-D35-based device, so that for the former, $J_{sc} = 10.80 \text{ mA cm}^{-2}$ is higher. For both of

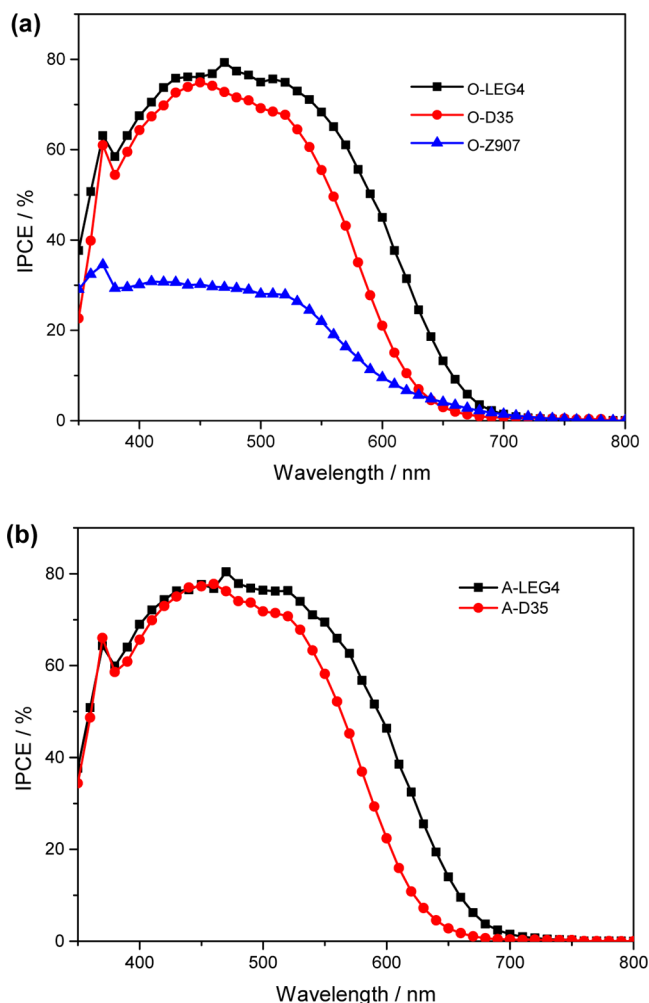


Figure 5. IPCE spectra of the devices based on three dyes and PEDOT from PEP of *bis*-EDOT in organic (a) and aqueous (b) electrolyte.

them, the IPCE is more than two times higher than that of the IPCE of cell O-(Ru-Z907) (35% at 500 nm). These values agree with the J_{sc} values shown in Table 2 above.

In Figure 5b, a similar IPCE trend was observed for PEDOT prepared from aqueous solutions. For A-LEG4 and A-D35, a similar maximum IPCE value of 80% was obtained, while the broader absorption of A-LEG4 than A-D35 agrees well with higher $J_{sc} = 10.94 \text{ mA cm}^{-2}$ for A-LEG4.

Figure SI-2 of the Supporting Information shows the light absorbance spectra of three dyes, LEG4, D35, and Z907, as sensitizer of a $2 \mu\text{m}$ thick TiO_2 film. The absorption edges of LEG4, D35, and Ru-Z907 are 670 , 650 , and 750 nm , respectively. However, dyes D35 and LEG4 have an absorbance higher than that of Ru-Z907, conforming to the fact that metal-free organic sensitizers have in general a higher extinction coefficient with respect to Ru coordination complex sensitizers. From the UV–vis absorption curve and IPCE spectra, it is indicated that D- π -A sensitizers D35 and LEG4 not only can absorb more light but also are more efficient in photon-to-current conversion efficiency than Ru-Z907. Therefore, these organic metal-free D- π -A sensitizers are more suitable for efficient conducting polymer-based ssDSCs.

3.5. Electron Lifetime Measurement. To investigate the remarkable difference in V_{oc} among different devices, the

interfacial charge recombination was studied. In ssDSCs, the V_{oc} is determined by the difference between the Fermi level of TiO_2 and the HOMO level of HTM. Charge recombination is one of the most critical charge losses. The main recombination process is due to the fact that the injected electrons on the conduction band of TiO_2 can recombine with the oxidized HTM, doped PEDOT in the present case, or eventually the oxidized sensitizer, rather than be collected to the FTO substrate and contribute to photocurrent generation in the external circuit.

In Figure 6a, the electron lifetimes of different dye-sensitized devices using PEDOT from *bis*-EDOT are plotted versus V_{oc} . It

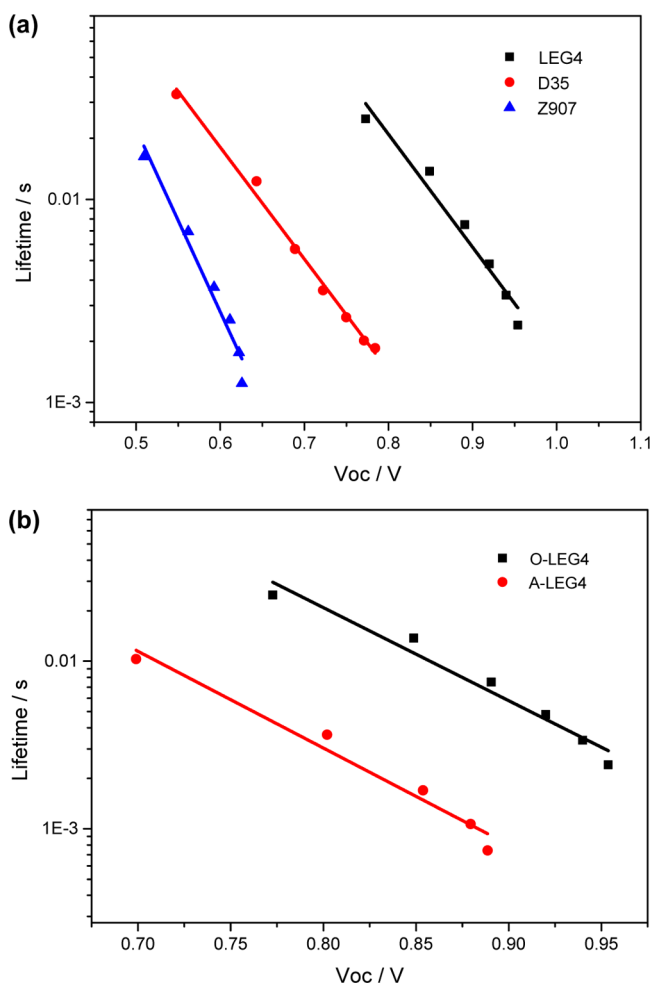


Figure 6. (a) Electron lifetime of three dye-sensitized devices versus open-circuit potential using PEDOT from organic PEP of *bis*-EDOT; (b) electron lifetime of aqueous and nonaqueous polymerized PEDOT-based devices using LEG4 dye.

can be seen that the lifetime of O-LEG4 is much longer than that of O-D35 and O-Z907, which is compatible with the V_{oc} values obtained in three dye-based devices, shown in Table 2. Because LEG4 and D35 have alkyl chains to block the charge recombination more efficiently than Ru-Z907, the organic dye-based solar cells work better than Ru-Z907-based solar cells. In Figure 6b, the electron lifetime of O-LEG4 and A-LEG4 devices were investigated, and it is shown that O-LEG4 has much longer lifetime than A-LEG4, which is also confirmed with the lower V_{oc} for the A-LEG4-based device. The electron lifetime difference reflects recombination for devices based on

aqueous PEP that is faster than that of those based on organic PEP. The faster charge recombination for A-LEG4 than O-LEG4 could arise from the fact that shorter chain length but a greater number of chains of PEDOT are generated in aqueous medium than in organic medium PEP, leading to more holes at the interface between dyes and HTMs and thus more charge recombination. The details of this assumption will be discussed in Section 3.8.

3.6. UV–Vis–NIR Spectroscopy Measurement. The differences in the solar cell performance in the two cases of nonaqueous and aqueous PEP will undoubtedly be related to the nature of the corresponding PEDOT. To obtain direct information on the different properties of PEDOT generated from aqueous and organic PEP, and to make it clear for the understanding on the mechanism of PEP, UV–vis–NIR spectra of PEDOT films were investigated. In this measurement, the samples were prepared following the procedure that was the same as that for fabrication of solar cell devices, without either post-treatment or Ag deposition. Three types of films, TiO_2 /D35, TiO_2 /D35/O-PEDOT, and TiO_2 /D35/A-PEDOT, are discussed here. The wavelength was chosen from 700 to 2000 nm because D35 has no absorption in this range. Figure 7

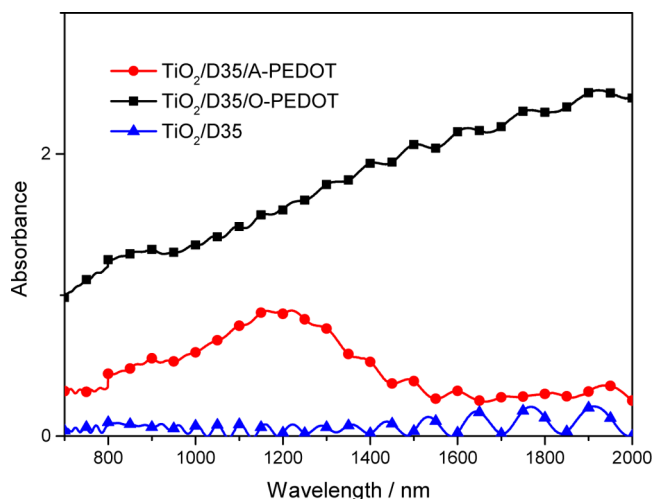


Figure 7. Light absorption spectra of TiO_2 /D35, TiO_2 /D35/O-PEDOT, and TiO_2 /D35/A-PEDOT films. PEDOT is generated from PEP by using the chronopotentiometry method.

shows the absorption of the films with and without PEDOT obtained by using a constant current (chronopotentiometry) PEP method. As expected, the film TiO_2 /D35 shows nearly zero absorption from 700 to 2000 nm. The oscillating (interference) fluctuations superimposed on the spectrum are due to the thickness of the electrode film. However, in the presence of PEDOT, the films show strong absorption in different ranges, depending on aqueous or nonaqueous preparation. Specifically, TiO_2 /D35/O-PEDOT has a small absorption peak at 850 nm and a continuously increased absorption from 1000 to 2000 nm. In contrast, TiO_2 /D35/A-PEDOT exhibited an obviously distinct absorption behavior, with a broad peak absorption from 1000 to 1400 nm and without any absorption above 1500 nm.

The optical response of the conducting polymer is directly related to its doping state. During the process of oxidation of the precursor or shorter oligomers followed by coupling, the electrochemical driving force for doping is lower than that for

polymer formation, and the polymer remains doped after the PEP has been terminated. There are two possible forms for doping charges of conducting polymer PEDOT, namely, the polaron (PEDOT⁺) and the bipolaron (PEDOT²⁺), depending on the chemical structure of the polymer and its doping level. At high doping levels, the bipolaron band will be formed, which is characterized by a broad absorption in near IR region.⁴⁹

On the one hand, TiO₂/D35/O-PEDOT shows an increasing and continuous absorption at a broad wavelength range from 700 to 2000 nm, thereby indicating that the electronic structure of O-PEDOT polymer has a bi(polarons) band-related features and a relatively high doping level. It can be expected that a highly delocalized conformation from O-PEDOT can be obtained during organic-based PEP. The highly delocalized structure is possibly related to the long polymer chains, as further discussed in Section 3.8.

On the other hand, a surprising behavior was observed for A-PEDOT. It showed increased absorption from 700 to 1200 nm and a significantly decreased absorption from 1200 to 2000 nm. This absorption peak around 1200 nm could be related to the electronic structure of polaron or bipolaron.⁴⁹ It could be attributed to a less-delocalized structure with shorter chains for A-PEDOT than for O-PEDOT.

By comparison of the two cases above, the assumptions that O-PEDOT has a much higher delocalized conformation and better chain organization than A-PEDOT, could also be supported by the SEM pictures of polymers obtained from organic and aqueous media, as shown in Figure SI-3 of the Supporting Information. PEDOT with a smooth and compact structure was formed from organic-based polymerization, but PEDOT with a porous and rough morphology was obtained from aqueous polymerization. This is in agreement with the results reported by Lacaze et al.³⁶ in which the PEDOT film morphologies investigated by atomic force microscopy showed columnar structure for films performed in aqueous micellar medium and smooth compact structure for films performed in organic medium.

3.7. Hole Conductivity and Hole Mobility Measurement. In competition with charge recombination, charge separation plays an important role in the energy conversion efficiency. After dye regeneration, the holes should be transported away through the HTM when injected electrons move away through n-type semiconductor TiO₂. The space-charge-limited current (SCLC) method was used to measure hole mobility.^{50–52} The corresponding films were prepared by following the procedure used for device fabrication. In the SCLC method, the current density J is limited by the space charge if the contacts are ohmic and any trapped states are filled. The expression for current density versus potential (valid for thin films, $L \gg d$) is given as

$$J = \frac{2}{\pi} \mu \epsilon_r \epsilon_0 \frac{V^2}{L^2}$$

where ϵ_r is the dielectric constant of the material (3 for organic semiconductor), μ the hole mobility, V the applied voltage, and L the distance between the two Ag electrodes (0.2 cm). L is much longer than the thickness d of the PEDOT film, so the equation above is valid to evaluate the hole mobility.⁵² When the current–voltage curves and square root of current density–voltage curves are plotted, as shown in Figure SI-4 of the Supporting Information, the detailed hole conductivity and mobility values expressed in Table 4 are derived.

Table 4. Hole Mobility and Conductivity of D35/O-PEDOT and D35/A-PEDOT in ssDSC

	hole conductivity (S cm ⁻¹)	hole mobility (cm (Vs) ⁻¹)
O-PEDOT	6.7×10^{-3}	2.0×10^{-4}
A-PEDOT	2.0×10^{-4}	1.25×10^{-5}

It can be seen that the hole conductivity and hole mobility of O-PEDOT film are 6.7×10^{-3} S cm⁻¹ and 2.0×10^{-4} cm (Vs)⁻¹, respectively, which are much higher than those in A-PEDOT, 2.0×10^{-4} S cm⁻¹ and 1.25×10^{-5} cm (Vs)⁻¹, demonstrating that O-PEDOT can transport holes faster. In addition, the higher hole conductivity and mobility for O-PEDOT than for A-PEDOT match well with the more smooth and delocalized structure of O-PEDOT, shown in Figure SI-3 of the Supporting Information. Moreover, O-PEDOT with high hole mobility can decrease the charge transport resistance in the device, improving the fill factor of the corresponding device.

3.8. Photoinduced Absorption Spectroscopy. To further evaluate the aforementioned assumptions, photoinduced absorption spectra of different films with and without PEDOT were investigated. Here, PIA spectroscopy is mainly used to study the regeneration process of oxidized dye molecules by the hole-conducting polymer, following the electron injection from oxidized dye to the conduction band of TiO₂.⁵² In Figure 8, a TiO₂/LEG4 film showed two parts of

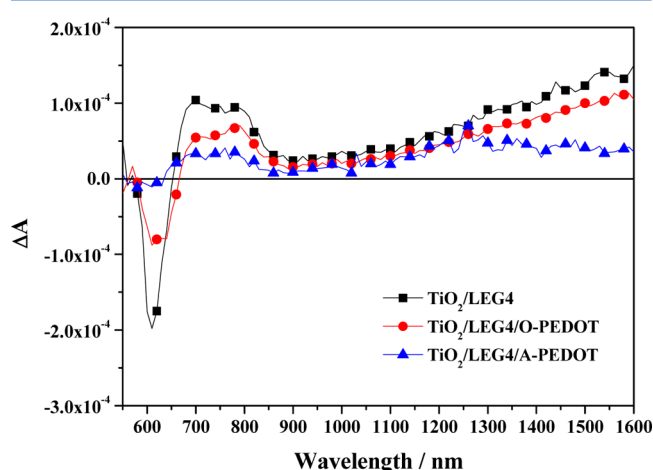


Figure 8. PIA signals of LEG4-sensitized TiO₂ films with and without PEDOT, by organic PEP and aqueous PEP.

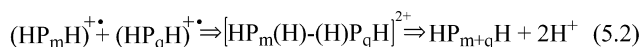
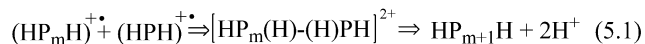
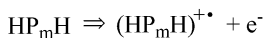
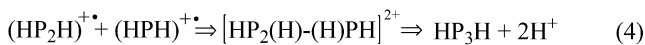
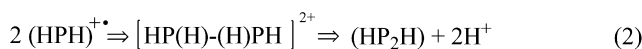
absorption which arise from the oxidized state of LEG4 and the polymer. One part is in the range from 700 to 850 nm, and the other one is located in a broad range above 1000 nm. After deposition of PEDOT on the TiO₂/LEG4 film, the oxidized LEG4, following excitation by light, can be regenerated by PEDOT. The decreased intensity of absorption in both regions is attributed to the dye regeneration process. Therefore, the doped state of PEDOT can also contribute to the light absorption in NIR regions, as can be seen in Figure 7a,b. Therefore, it is preferred to compare the absorption intensity change at shorter wavelengths, below 1000 nm, rather than in the NIR region, taking into account that PEDOT contributes much less absorption in the range from 700 to 800 nm. By comparison of different curves in Figure 8, it is clearly seen that in both cases of polymers derived from O-PEP and A-PEP the absorption intensity at 700–800 nm decreased because of dye regeneration. However, a more pronounced decrease occurred

in the case of the A-PEDOT-based film. Thereby, it can be assumed that faster dye regeneration occurs by deposition of A-PEDOT than by that of O-PEDOT. Moreover, the PIA absorption curves on $\text{TiO}_2/\text{LEG4}/\text{A-PEDOT}$ and $\text{TiO}_2/\text{LEG4}/\text{O-PEDOT}$ after regeneration match well with the shape of UV-vis-NIR absorption on A-PEDOT and O-PEDOT, which can indirectly certify the different properties of the polymer in the two cases. In Figure SI-5 of the Supporting Information, PIA signals of $\text{TiO}_2/\text{D35}$, $\text{TiO}_2/\text{D35}/\text{O-PEDOT}$, and $\text{TiO}_2/\text{D35}/\text{A-PEDOT}$, are presented. They showed the same trend as LEG4-based films. A-PEDOT can contribute an extent of regeneration higher than that of O-PEDOT.

The faster dye regeneration process in A-PEDOT-based devices could be attributed to the different structures of polymers obtained from the two media. On one hand, a rough and porous PEDOT film is generated from aqueous PEP. Additionally, a less delocalized PEDOT with short chain length could be expected for A-PEDOT. We suggest that the micelles and the low concentration of the precursor form a more porous structure as well as shorter polymer chains in aqueous PEP. However, the same amount of PEDOT material should be formed in the pores of TiO_2 in aqueous electrolyte-based PEP because the amount of charge controlled during PEP was the same as that in the organic medium. As a result, for the same applied charge, a smaller amount of polymer chains, but longer polymer chains, could be grown inside the TiO_2 pores when using organic PEP. Thus, the high amount of porous A-PEDOT with shorter chains could have a higher contact area with dye molecules on the surface of porous TiO_2 , resulting in the faster dye regeneration process.

3.9. Mechanisms of PEP of Precursor. The mechanism for PEP in different media is discussed in Scheme 1. HPH represents the precursor, i.e., either EDOT monomer or *bis*-EDOT dimer.

Scheme 1. Mechanism of the Photoelectrochemical Polymerization Process



.....



First, when the TiO_2/dye electrode is illuminated, dye molecules will be excited and inject electrons into TiO_2 , leaving holes in the oxidized form of the dye; these holes tend to oxidize the precursor (HPH) in the surroundings, and the oxidized state $(\text{HPH})^{+\bullet}$ will be created (step 1). Then, the coupling of two $(\text{HPH})^{+\bullet}$ species proceeds so that dimer HP_2H , (step 2) is generated. Further, upon electrode illumination, not only the monomer but also the dimer HP_2H will be oxidized to $(\text{HP}_2\text{H})^{+\bullet}$ (step 3). This process is

much easier than the oxidation for precursor because dimer HP_2H has an oxidation potential lower than that of HPH. The oxidized state of precursor dimer $(\text{HP}_2\text{H})^{+\bullet}$ will couple with $(\text{HPH})^{+\bullet}$ to give precursor trimer, HP_3H (step 4). Similar considerations are valid for oligomers (steps 5.1 and 5.2). For the oligomer with m ($m > 2$) precursor units, after its oxidation $(\text{HP}_m\text{H})^{+\bullet}$ (step 5), there are different ways to continue coupling. One possibility is to couple with $(\text{HPH})^{+\bullet}$, resulting in an oligomer with $(m + 1)$ units (step 5.1). Another possibility is to couple with another oligomer $(\text{HP}_q\text{H})^{+\bullet}$ so that longer chains HP_{m+q}H are created (step 5.2).

For the PEP in organic medium, the concentration of precursor is 10 mM. Therefore, a sufficiently high number of precursor molecules are available in the pores to come into contact with dye molecules. After illumination, a large amount of $(\text{HPH})^{+\bullet}$ is created during the photo-oxidation process on the surface of the dye/ TiO_2 working electrode. As a result, upon further polymerization, the oligomer species $(\text{HP}_m\text{H})^{+\bullet}$ has more chances to couple with a unit of oxidized precursor $(\text{HPH})^{+\bullet}$. Therefore, this process is easy to proceed because of the high concentration of precursor, so that a regular, smooth, ordered and, finally, highly doped polymer with longer chains is formed.

In contrast, in an aqueous electrolyte, micelles are introduced into the system by adding a surfactant, e.g., TritonX-100, to enhance the precursor solubility. However, the concentration of precursor is usually much lower than that in organic medium (< 1 mM, in the case of *bis*-EDOT). Moreover, in the aqueous phase, the precursor is incorporated into the micelles, and the formation of a micellar cage can cause a structure restriction on the polymer. In each cage, the oligomer starts to couple with the precursor to form polymer chains with variant orientation. Finally, a rough and porous PEDOT will be generated in the aqueous phase. Also, a PEDOT with short chains but a high number of pieces will be expected to generate from aqueous PEP because of the micellar cage restriction.

Therefore, because of the porous and disordered morphology and the high amount of short chains of A-PEDOT, the generated polymer A-PEDOT can have a contact area that is larger than that of the O-PEDOT system, with more holes at the interface between the dye molecules on the porous TiO_2 surface and HTM, causing an efficient dye regeneration. Unfortunately, the injected electrons on the conduction band of TiO_2 will also have more chances to recombine with the holes on porous A-PEDOT, resulting in faster charge recombination. In contrast, with the observation of a higher degree of delocalized electrons in O-PEDOT, we expect and also experimentally confirmed (Section 3.7) better hole conductivity, which will reduce the charge transport resistance in the device, leading to an improved fill factor. On the other hand, because of the longer but smaller amount of chains, a relatively slower charge recombination can be expected. Therefore, O-PEDOT-based devices exhibit a electron lifetime much longer than that of A-PEDOT-based devices.

4. CONCLUSION

Donor- π -acceptor (D- π -A) sensitizers were employed in this work for photoelectrochemical polymerization because of their appropriate energy levels and good light absorption ability. Conducting polymer PEDOT generated both from *bis*-EDOT and EDOT as precursors was used as hole-transporting material in solid-state dye-sensitized solar cells. The aqueous PEP approach, as a cost-effective and environmentally friendly

method, was employed to reduce the oxidation potential of the precursor. The PEDOT-based device, obtained by aqueous PEP of precursor *bis*-EDOT, exhibits the impressive power conversion efficiency of 5.2%, comparable with the 5.6% of the device based on PEDOT from organic PEP of *bis*-EDOT. Moreover, the less expensive precursor monomeric EDOT was for the first time used in the PEP process for dye solar cells, in both organic and aqueous electrolyte. The device based on PEDOT obtained from PEP of EDOT in aqueous electrolyte showed 3.0% efficiency, much higher than the one based on PEDOT from PEP of EDOT in organic medium. A possible mechanism, corroborated by spectroscopic measurement, was proposed on the basis of the morphologies of polymers and the performance in the two kinds of devices. In aqueous medium, it is proposed that the PEP leads to PEDOT with a porous and rough structure, and a high amount of short chains mainly inside the TiO₂ pores; whereas in the case of organic medium, PEP leads to polymers with a smooth and compact morphology showing high delocalized charge and lower amount of longer chains. This differentiation could cause faster dye regeneration for A-PEDOT-based devices, whereas we obtain higher mobility and less charge recombination for O-PEDOT devices. For future improvement, the combination of the two positive effects from the aqueous and the organic PEP could contribute to solid-state dye-sensitized solar cells with higher efficiency.

■ ASSOCIATED CONTENT

■ Supporting Information

Information on detailed cyclic voltammetry curves of precursors *bis*-EDOT and EDOT and dye molecules LEG4, D35, Z907 in organic and aqueous media; UV-vis spectroscopy of different dyes; UV-vis-NIR spectroscopy of polymer films; PIA signals of D35-sensitized TiO₂ films with and without PEDOT; SEM images of PEDOT from aqueous and nonaqueous PEP. This material is available free of charge via the Internet at <http://pubs.acs.org>.

■ AUTHOR INFORMATION

Corresponding Author

*E-mail: nikolaos@kemi.uu.se.

Author Contributions

#These authors contributed to this work equally.

Notes

The authors declare no competing financial interest.

■ ACKNOWLEDGMENTS

Financial assistance has been provided by the Swedish Energy Agency, the STandUP for Energy program, the Swedish Research Council (VR), the Knut and Alice Wallenberg Foundation and the French-Swedish Research Mobility Program "Gustaf Dalén" (Swedish Foundation for Strategic Research application number IMF11-0060; France No.26224RH). Jinbao Zhang gratefully acknowledges the China Scholarship Council (CSC) for a PhD study fellowship. The authors thank Dr. Hélène Lecoq, Engineer (ITODYS) for SEM images.

■ REFERENCES

- (1) Desilvestro, J.; Grätzel, M.; Kavan, L.; Moser, J.; Augustynski, J. Highly Efficient Sensitization of Titanium-Dioxide. *J. Am. Chem. Soc.* **1985**, *107*, 2988–2990.
- (2) Vlachopoulos, N.; Liska, P.; Augustynski, J.; Grätzel, M. Very Efficient Visible Light Energy Harvesting and Conversion by Spectral Sensitization of High Surface-Area Polycrystalline Titanium-Dioxide Films. *J. Am. Chem. Soc.* **1988**, *110*, 1216–1220.
- (3) Oregan, B.; Grätzel, M. A Low-Cost, High-Efficiency Solar-Cell Based on Dye-Sensitized Colloidal TiO₂ Films. *Nature (London, U.K.)* **1991**, *353*, 737–740.
- (4) Hagfeldt, A.; Boschloo, G.; Sun, L. C.; Kloo, L.; Pettersson, H. Dye-Sensitized Solar Cells. *Chem. Rev. (Washington, DC, U.S.)* **2010**, *110*, 6595–6663.
- (5) Hagfeldt, A.; Grätzel, M. Light-Induced Redox Reactions in Nanocrystalline Systems. *Chem. Rev. (Washington, DC, U.S.)* **1995**, *95*, 49–68.
- (6) Humphry-Baker, N.; Driscoll, K.; Rao, A.; Torres, T.; Snaith, H. J.; Friend, R. H. Time-Evolution of Poly(3-hexylthiophene) as an Energy Relay Dye in Dye-Sensitized Solar Cells. *Nano Lett.* **2012**, *12*, 634–639.
- (7) Feldt, S. M.; Cappel, U. B.; Johansson, E. M. J.; Boschloo, G.; Hagfeldt, A. Characterization of Surface Passivation by Poly-(methylsiloxane) for Dye-Sensitized Solar Cells Employing the Ferrocene Redox Couple. *J. Phys. Chem. C* **2010**, *114*, 10551–10558.
- (8) Yella, A.; Lee, H. W.; Tsao, H. N.; Yi, C. Y.; Chandiran, A. K. Porphyrin-Sensitized Solar Cells with Cobalt (II/III)-Based Redox Electrolyte Exceed 12% Efficiency (vol 334, pg 629, 2011). *Science* **2011**, *334*, 1203–1203.
- (9) Chiba, Y.; Islam, A.; Komiya, R.; Koide, N.; Han, L. Y. Conversion Efficiency of 10.8% by a Dye-Sensitized Solar Cell Using a TiO₂ Electrode with High Haze. *Appl. Phys. Lett.* **2006**, *88*, 223505.
- (10) Mathew, S.; Yella, A.; Gao, P.; Humphry-Baker, R.; Curchod, B. F.; Ashari-Astani, N.; Tavernelli, I.; Rothlisberger, U.; Nazeeruddin, M. K.; Grätzel, M. Dye-Sensitized Solar Cells with 13% Efficiency Achieved Through the Molecular Engineering of Porphyrin Sensitizers. *Nat. Chem.* **2014**, *6*, 242–247.
- (11) Bach, U.; Lupo, D.; Comte, P.; Moser, J. E.; Weissortel, F.; Salbeck, J.; Spreitzer, H.; Grätzel, M. Solid-State Dye-Sensitized Mesoporous TiO₂ Solar Cells with High Photon-to-Electron Conversion Efficiencies. *Nature (London, U.K.)* **1998**, *395*, 583–585.
- (12) Saito, Y.; Kitamura, T.; Wada, Y.; Yanagida, S. Application of Poly(3,4-ethylenedioxythiophene) to Counter Electrode in Dye-Sensitized Solar Cells. *Chem. Lett.* **2002**, *31*, 1060–1061.
- (13) Tennakone, K.; Kumara, G. R. R. A.; Kumarasinghe, A. R.; Wijayantha, K. G. U.; Sirimanne, P. M. A Dye-Sensitized Nano-Porous Solid-State Photovoltaic Cell. *Semicond. Sci. Technol.* **1995**, *10*, 1689–1693.
- (14) Cappel, U. B.; Gibson, E. A.; Hagfeldt, A.; Boschloo, G. Dye Regeneration by Spiro-MeOTAD in Solid State Dye-Sensitized Solar Cells Studied by Photoinduced Absorption Spectroscopy and Spectroelectrochemistry. *J. Phys. Chem. C* **2009**, *113*, 6275–6281.
- (15) Burschka, J.; Dualeh, A.; Kessler, F.; Baranoff, E.; Cevey-Ha, N. L.; Yi, C. Y.; Nazeeruddin, M. K.; Grätzel, M. Tris(2-(1H-pyrazol-1-yl)pyridine)cobalt(III) as p-Type Dopant for Organic Semiconductors and Its Application in Highly Efficient Solid-State Dye-Sensitized Solar Cells. *J. Am. Chem. Soc.* **2011**, *133*, 18042–18045.
- (16) Snaith, H. J.; Grätzel, M. Electron and Hole Transport Through Mesoporous TiO₂ Infiltrated with Spiro-MeOTAD. *Adv. Mater.* **2007**, *19*, 3643–3647.
- (17) Zhang, W.; Zhu, R.; Li, F.; Wang, Q.; Liu, B. High-Performance Solid-State Organic Dye Sensitized Solar Cells with P3HT as Hole Transporter. *J. Phys. Chem. C* **2011**, *115*, 7038–7043.
- (18) Yang, L.; Xu, B.; Bi, D. Q.; Tian, H. N.; Boschloo, G.; Sun, L. C.; Hagfeldt, A.; Johansson, E. M. J. Initial Light Soaking Treatment Enables Hole Transport Material to Outperform Spiro-OMeTAD in Solid-State Dye-Sensitized Solar Cells. *J. Am. Chem. Soc.* **2013**, *135*, 7378–7385.
- (19) Song, I. Y.; Park, S. H.; Lim, J.; Kwon, Y. S.; Park, T. A Novel Hole Transport Material for Iodine-Free Solid State Dye-Sensitized Solar Cells. *Chem. Commun. (Cambridge, U.K.)* **2011**, *47*, 10395–10397.

- (20) Xu, B.; Tian, H. N.; Bi, D. Q.; Gabrielsson, E.; Johansson, E. M. J.; Boschloo, G.; Hagfeldt, A.; Sun, L. C. Efficient Solid State Dye-Sensitized Solar Cells Based on an Oligomer Hole Transport Material and an Organic Dye. *J. Mater. Chem. A* **2013**, *1*, 14467–14470.
- (21) Zhang, J.; Haggman, L.; Jouini, M.; Jarboui, A.; Boschloo, G.; Vlachopoulos, N.; Hagfeldt, A. Solid-State Dye-Sensitized Solar Cells Based on Poly(3,4-ethylenedioxythiophene) and Metal-Free Organic Dyes. *ChemPhysChem* **2014**, *15*, 1043–1047.
- (22) Zhang, W.; Cheng, Y. M.; Yin, X. O.; Liu, B. Solid-State Dye-Sensitized Solar Cells with Conjugated Polymers as Hole-Transporting Materials. *Macromol. Chem. Phys.* **2011**, *212*, 15–23.
- (23) Saito, Y.; Fukuri, N.; Senadeera, R.; Kitamura, T.; Wada, Y.; Yanagida, S. Solid State Dye Sensitized Solar Cells Using In Situ Polymerized PEDOTs as Hole Conductor. *Electrochem. Commun.* **2004**, *6*, 71–74.
- (24) Xia, J. B.; Masaki, N.; Lira-Cantu, M.; Kim, Y.; Jiang, K. J.; Yanagida, S. Influence of Doped Anions on Poly(3,4-ethylenedioxythiophene) as Hole Conductors for Iodine-Free Solid-State Dye-Sensitized Solar Cells. *J. Am. Chem. Soc.* **2008**, *130*, 1258–1263.
- (25) Liu, X. Z.; Zhang, W.; Uchida, S.; Cai, L. P.; Liu, B.; Ramakrishna, S. An Efficient Organic-Dye-Sensitized Solar Cell with In Situ Polymerized Poly(3,4-ethylenedioxythiophene) as a Hole-Transporting Material. *Adv. Mater.* **2010**, *22*, E150–E155.
- (26) Saito, Y.; Kitamura, T.; Wada, Y.; Yanagida, S. Poly(3,4-ethylenedioxythiophene) as a Hole Conductor in Solid State Dye Sensitized Solar Cells. *Synth. Met.* **2002**, *131*, 185–187.
- (27) Liu, X. Z.; Cheng, Y. M.; Wang, L.; Cai, L. P.; Liu, B. Light Controlled Assembling of Iodine-Free Dye-Sensitized Solar Cells with Poly(3,4-ethylenedioxythiophene) as a Hole Conductor Reaching 7.1% Efficiency. *Phys. Chem. Chem. Phys.* **2012**, *14*, 7098–7103.
- (28) Cai, L. P.; Liu, X. Z.; Wang, L.; Liu, B. Iodine-Free Organic Dye Sensitized Solar Cells with In Situ Polymerized Hole Transporting Material from Alkoxy-Substituted TriEDOT. *Polym. Bull.* **2012**, *68*, 1857–1865.
- (29) Yang, L.; Zhang, J. B.; Shen, Y.; Park, B. W.; Bi, D. Q.; Haggman, L.; Johansson, E. M. J.; Boschloo, G.; Hagfeldt, A.; Vlachopoulos, N.; et al. New Approach for Preparation of Efficient Solid-State Dye-Sensitized Solar Cells by Photoelectrochemical Polymerization in Aqueous Micellar Solution. *J. Phys. Chem. Lett.* **2013**, *4*, 4026–4031.
- (30) Ellis, H.; Eriksson, S. K.; Feldt, S. M.; Gabrielsson, E.; Lohse, P. W.; Lindblad, R.; Sun, L. C.; Rensmo, H.; Boschloo, G.; Hagfeldt, A. Linker Unit Modification of Triphenylamine-Based Organic Dyes for Efficient Cobalt Mediated Dye-Sensitized Solar Cells. *J. Phys. Chem. C* **2013**, *117*, 21029–21036.
- (31) Murakoshi, K.; Kogure, R.; Wada, Y.; Yanagida, S. Solid State Dye-Sensitized TiO₂ Solar Cell with Polypyrrole as Hole Transport Layer. *Chem. Lett.* **1997**, *26*, 471–472.
- (32) Kitamura, T.; Maitani, M.; Matsuda, M.; Wada, Y.; Yanagida, S. Improved Solid-State Dye Solar Cells with Polypyrrole Using a Carbon-Based Counter Electrode. *Chem. Lett.* **2001**, *30*, 1054–1055.
- (33) Mozer, A. J.; Wada, Y.; Jiang, K. J.; Masaki, N.; Yanagida, S.; Mori, S. N. Efficient Dye-Sensitized Solar Cells Based on a 2-Thiophen-2-yl-vinyl-conjugated Ruthenium Photosensitizer and a Conjugated Polymer Hole Conductor. *Appl. Phys. Lett.* **2006**, *89*, 043509.
- (34) Mozer, A. J.; Panda, D. K.; Gambhir, S.; Romeo, T. C.; Winther-Jensen, B.; Wallace, G. G. Flexible and Compressible GoreTex-PEDOT Membrane Electrodes for Solid-State Dye-Sensitized Solar Cells. *Langmuir* **2010**, *26*, 1452–1455.
- (35) Mozer, A. J.; Panda, D. K.; Gambhir, S.; Winther-Jensen, B.; Wallace, G. G. Microsecond Dye Regeneration Kinetics in Efficient Solid State Dye-Sensitized Solar Cells Using a Photoelectrochemically Deposited PEDOT Hole Conductor. *J. Am. Chem. Soc.* **2010**, *132*, 9543–9545.
- (36) Sakmeche, N.; Aeiyaeh, S.; Aaron, J. J.; Jouini, M.; Lacroix, J. C.; Lacaze, P. C. Improvement of the Electrosynthesis and Physicochemical Properties of Poly(3,4-ethylenedioxythiophene) Using a Sodium Dodecyl Sulfate Micellar Aqueous Medium. *Langmuir* **1999**, *15*, 2566–2574.
- (37) Sakmeche, N.; Aaron, J. J.; Dieng, M.; Jouini, M.; Aeiyaeh, S.; Lacroix, J. C.; Lacaze, P. C. Deposition on Oxidizable Metals of Poly[3,4-dioxyethylenethiophene] Films Electrosynthesized in Micellar Aqueous Media. *J. Chim. Phys. Phys.-Chim. Biol.* **1998**, *95*, 1531–1534.
- (38) Sakmeche, N.; Aaron, J. J.; Fall, M.; Aeiyaeh, S.; Jouini, M.; Lacroix, J. C.; Lacaze, P. C. Anionic Micelles; A New Aqueous Medium for Electropolymerization of Poly(3,4-ethylenedioxythiophene) Films on Pt Electrodes. *Chem. Commun. (Cambridge, U.K.)* **1996**, 2723–2724.
- (39) Sakmeche, N.; Bazzou, E. A.; Fall, M.; Aeiyaeh, S.; Jouini, M.; Lacroix, J. C.; Aaron, J. J.; Lacaze, P. C. Application of Sodium Dodecylsulfate (SDS) Micellar Solution as an Organized Medium for Electropolymerization of Thiophene Derivatives in Water. *Synth. Met.* **1997**, *84*, 191–192.
- (40) Lagrost, C.; Lacroix, J. C.; Aeiyaeh, S.; Jouini, M.; Chane-Ching, K. I.; Lacaze, P. C. Host-Guest Complexation: A New Strategy for Electrodeposition of Processable Polythiophene Composites from Aqueous medium. *Chem. Commun. (Cambridge, U.K.)* **1998**, 489–490.
- (41) Lagrost, C.; Lacroix, J. C.; Chane-Ching, K. I.; Jouini, M.; Aeiyaeh, S.; Lacaze, P. C. Host-Guest Complexation: A Strategy to Form Sexithiophene Exhibiting Self-Assembly Properties. *Adv. Mater.* **1999**, *11*, 664–667.
- (42) Ellis, H.; Vlachopoulos, N.; Haggman, L.; Perruchot, C.; Jouini, M.; Boschloo, G.; Hagfeldt, A. PEDOT Counter Electrodes for Dye-Sensitized Solar Cells Prepared by Aqueous Micellar Electrodeposition. *Electrochim. Acta* **2013**, *107*, 45–51.
- (43) Hagberg, D. P.; Jiang, X.; Gabrielsson, E.; Linder, M.; Marinado, T.; Brinck, T.; Hagfeldt, A.; Sun, L. C. Symmetric and Unsymmetric Donor Functionalization. Comparing Structural and Spectral Benefits of Chromophores for Dye-Sensitized Solar Cells. *J. Mater. Chem.* **2009**, *19*, 7232–7238.
- (44) Gabrielsson, E.; Ellis, H.; Feldt, S.; Tian, H. N.; Boschloo, G.; Hagfeldt, A.; Sun, L. C. Convergent/Divergent Synthesis of a Linker-Variety Series of Dyes for Dye-Sensitized Solar Cells Based on the D35 Donor. *Adv. Energy Mater.* **2013**, *3*, 1647–1656.
- (45) Cameron, P. J.; Peter, L. M. Characterization of Titanium Dioxide Blocking Layers in Dye-Sensitized Nanocrystalline Solar Cells. *J. Phys. Chem. B* **2003**, *107*, 14394–14400.
- (46) Pavlishchuk, V. V.; Addison, A. W. Conversion Constants for Redox Potentials Measured versus Different Reference Electrodes in Acetonitrile Solutions at 25 Degrees C. *Inorg. Chim. Acta* **2000**, *298*, 97–102.
- (47) Thornton, D. C.; Corby, K. T.; Spendel, V. A.; Jordan, J.; Robbat, A.; Rutstrom, D. J.; Gross, M.; Ritzler, G. Pretreatment and Validation Procedure for Glassy-Carbon Voltammetric Indicator Electrodes. *Anal. Chem.* **1985**, *57*, 150–155.
- (48) Boschloo, G.; Hagfeldt, A. Photoinduced Absorption Spectroscopy as a Tool in the Study of Dye-Sensitized Solar Cells. *Inorg. Chim. Acta* **2008**, *361*, 729–734.
- (49) Bubnova, O.; Crispin, X. Towards Polymer-Based Organic Thermoelectric Generators. *Energy Environ. Sci.* **2012**, *5*, 9345–9362.
- (50) Heeger, A. J. Semiconducting and Metallic Polymers: The Fourth Generation of Polymeric Materials (Nobel Lecture). *Angew. Chem., Int. Ed.* **2001**, *40*, 2591–2611.
- (51) Snaith, H. J.; Grätzel, M. Enhanced Charge Mobility in a Molecular Hole Transporter via Addition of Redox Inactive Ionic Dopant: Implication to Dye-Sensitized Solar Cells. *Appl. Phys. Lett.* **2006**, *89*, 262114.
- (52) Park, B. W.; Yang, L.; Johansson, E. M. J.; Vlachopoulos, N.; Chams, A.; Perruchot, C.; Jouini, M.; Boschloo, G.; Hagfeldt, A. Neutral, Polaron, and Bipolaron States in PEDOT Prepared by Photoelectrochemical Polymerization and the Effect on Charge Generation Mechanism in the Solid-State Dye-Sensitized Solar Cell. *J. Phys. Chem. C* **2013**, *117*, 22484–22491.